Kuramoto Model of Coupled Oscillators with Positive and Negative Coupling Parameters: An Example of Conformist and Contrarian Oscillators

Hyunsuk Hong[1] and Steven H. Strogatz[2]

[1]Department of Physics and Research Institute of Physics and Chemistry, Chonbuk National University, Jeonju 561-756, Korea
[2]Department of Mathematics, Cornell University, New York 14853, USA

(Received 2 November 2010; published 2 February 2011)

We consider a generalization of the Kuramoto model in which the oscillators are coupled to the mean field with random signs. Oscillators with positive coupling are ''conformists''; they are attracted to the mean field and tend to synchronize with it. Oscillators with negative coupling are ''contrarians''; they are repelled by the mean field and prefer a phase diametrically opposed to it. The model is simple and exactly solvable, yet some of its behavior is surprising. Along with the stationary states one might have expected (a desynchronized state, and a partially-synchronized state, with conformists and contrarians locked in antiphase), it also displays a traveling wave, in which the mean field oscillates at a frequency different from the population's mean natural frequency.

DOI: 10.1103/PhysRevLett.106.054102 PACS numbers: 05.45.Xt, 89.75.−k

Globally coupled phase oscillators have been used to model diverse self-synchronizing systems in physics, chemistry and biology [1]. In the simplest cases the coupling is uniform: all the oscillators interact with equal strength, as in the classic Kuramoto model

$$\dot{\phi}_i = \omega_i + \frac{K}{N}\sum_{j=1}^{N}\sin(\phi_j - \phi_i), \qquad i = 1, \ldots, N. \quad (1)$$

Here $\phi_i(t)$ is the phase of the ith oscillator at time t, and ω_i is its natural frequency, chosen at random from a unimodal, symmetric probability density $g(\omega)$. Kuramoto assumed the coupling strength K is positive, corresponding to an attractive interaction between the oscillators.

A natural generalization is to allow K to have either sign. There are various ways to do this while still retaining the simplifying assumption of infinite-range interactions [2]. Several authors, inspired by models of spin glasses [3], have examined the effects of replacing K with random positive and negative coupling terms K_{ij} inside the sum in Eq. (1). The matrix elements K_{ij} are usually assumed to be symmetric ($K_{ij} = K_{ji}$) and independently chosen from the same probability distribution. The resulting models show evidence of glassy behavior, but their dynamics are not yet well understood [4].

A second approach, motivated by neural networks with excitatory and inhibitory coupling [5], is to replace K with a random variable K_j inside the sum in Eq. (1), where $K_j > 0$ for excitatory neurons, and $K_j < 0$ for inhibitory neurons. Now the randomness is regarded as an intrinsic property of the oscillators themselves [6], rather than of the interactions between them (as in the glassy models). Thus the interactions between i and j need not be symmetric (unless K_i happens to equal K_j). Somewhat surprisingly, extending the Kuramoto model in this fashion yields nothing qualitatively new; the dynamics turn out to resemble those of the original model [7].

Here we explore a third possibility: we replace K by a random variable K_i outside the sum in Eq. (1). The effect is to endow the oscillators with two kinds of personalities. Those with $K_i > 0$ behave like conformists—they tend to fall in line with whatever rhythm has emerged in the population, whereas those with $K_i < 0$ are repelled by the prevailing rhythm and act like contrarians. In that sense the model is loosely analogous to sociophysical models of opinion formation [8]. It is also reminiscent of other two-population variants of the Kuramoto model, such as those involving two frequency distributions [9] or two levels of attractive coupling [10].

The collective rhythm in the model is quantified by the complex order parameter

$$Z = Re^{i\Phi} = \frac{1}{N}\sum_{j=1}^{N} e^{i\phi_j}, \quad (2)$$

where the amplitude $0 \le R \le 1$ measures the system's macroscopic coherence and Φ is the average phase. Then, by replacing K with K_i, we find that Eq. (1) reduces to

$$\dot{\phi}_i = \omega_i + K_i R\sin(\Phi - \phi_i), \qquad i = 1, \ldots, N. \quad (3)$$

Equation (3) shows that the model retains the mean-field character of the original Kuramoto model; all the oscillators effectively interact only through the mean-field variables R and Φ. Furthermore, the term $K_i R\sin(\Phi - \phi_i)$ highlights the difference between the two types of oscillators; it pulls the conformists toward the collective phase Φ but pushes the contrarians away toward $\Phi + \pi$. The resulting dynamics are a bit more subtle than that, however, because the nonidentical frequencies ω_i also play a crucial role.

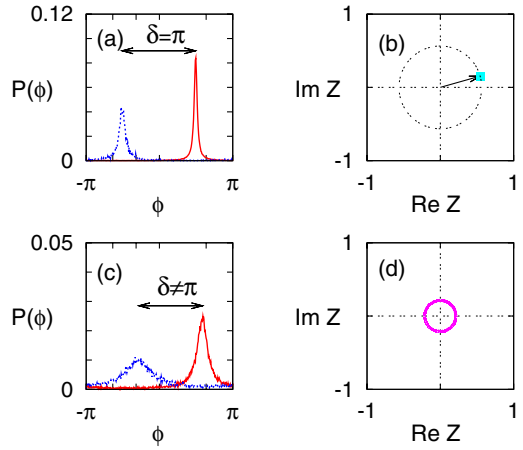

FIG. 1 (color online). The π state and traveling wave state. Parameters: $N = 25\,600$, $\gamma = 0.05$, $K_1 = -0.5$, $K_2 = 1.0$. (a) Phase distribution for the π state; the mean phase difference δ between the conformist (red) and contrarian (blue) oscillators is given by $\delta = \pi$. (b) The order parameter $Z(t)$ for the π-state corresponds to a fixed point. (c) Phase distribution for the traveling wave (TW) state; $\delta \neq \pi$. (d) The order parameter for the traveling wave state traces a circle, implying a nonzero mean phase velocity $\langle \dot{\phi}(t) \rangle \neq 0$.

To probe the system's long-term behavior, we performed numerical simulations. The ω_i were chosen at random from a Lorentzian probability density $g(\omega) = \gamma/[\pi(\omega^2 + \gamma^2)]$ of width γ and mean $\langle \omega \rangle = 0$ (the mean can be set to zero by choosing a suitable rotating frame). For simplicity we assumed a double-δ distribution of coupling strengths: $\Gamma(K) = (1 - p)\delta(K - K_1) + p\delta(K - K_2)$, where $K_1 < 0$ and $K_2 > 0$ represent the couplings for the contrarians and conformists, respectively, and p denotes the probability that a random oscillator is a conformist. Equation (3) was integrated using Heun's method with a time step $\delta t = 0.01$ for 10^5 time steps. The initial 90% of each run was discarded as a transient, after which all quantities of interest were measured.

The system always settles into one of three kinds of long-term behavior, depending on the parameters and initial conditions: (i) *Incoherent state*: The oscillators are completely desynchronized and scattered uniformly across all phases. (ii) *π-state*: The conformist oscillators converge to a partially synchronized state [1], as do the contrarian oscillators. Both generate stationary distributions of phases. The peaks of the distributions, as one would expect, are diametrically opposed, separated by an angle $\delta = \pi$, as shown in Fig. 1(a). Because both distributions are stationary, the order parameter $Z(t)$ remains motionless when plotted in the complex plane [Fig. 1(b)]. (iii) *Traveling wave state*: The phase distributions spontaneously travel at constant speed along the phase axis, always maintaining a constant separation $\delta \neq \pi$ [Fig. 1(c)]. As a result, the order parameter $Z(t)$ traces a circle about the origin at constant angular velocity, as shown in Fig. 1(d).

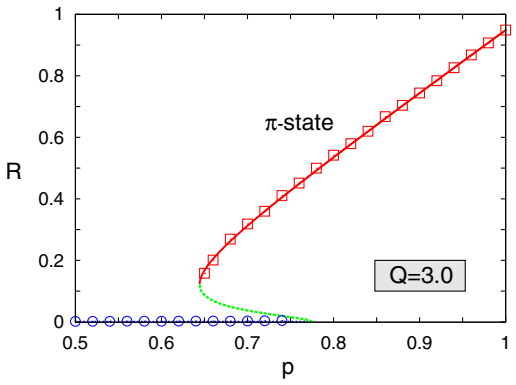

FIG. 2 (color online). Order parameter R vs p for $Q = 3$, computed by numerical integration (symbols) and compared to theoretical prediction from Eq. (11) (lines). Solid lines, stable states; dotted line, unstable π state. Stable π states were found numerically by integrating from the in-phase initial condition $\phi_i(0) = 0$ for all i, for each p. Stable incoherent states were found by integrating from random initial conditions. Parameters: $N = 25600$, $\gamma = 0.05$, $K_1 = -3.0$, $K_2 = 1.0$.

Figs. 2 and 3 show the transitions among these states as we vary p (the proportion of conformists). The results divide into two cases, depending on whether the conformists or the contrarians are more strongly affected by the mean field.

Figure 2 shows what happens when the contrarians are more strongly affected, in the sense that $Q \equiv -K_1/K_2 > 1$. As we increase p from 0, the system starts out incoherent, which makes intuitive sense: for small p, the system is dominated by contrarians who (of course) cannot agree on anything. But once p exceeds a certain threshold, there are enough conformists around for a consensus to emerge. At that point the system jumps discontinuously up to the π state, where it is polarized into two camps. Whatever the conformists decide on, the contrarians

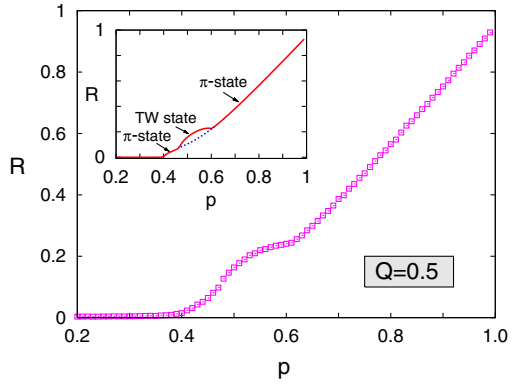

FIG. 3 (color online). Order parameter R vs p for $Q = 0.5$, computed by numerical integration. Inset shows theoretical prediction from Eq. (11). Red solid line, stable states; blue dotted line, unstable state. Parameters: $N = 25\,600$, $\gamma = 0.05$, $K_1 = -0.5$, $K_2 = 1.0$.

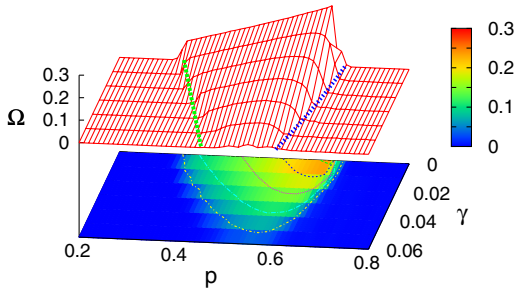

FIG. 4 (color online). Wave speed Ω as a function of γ and p for $Q = 0.5$. The data are also plotted as a contour map, with heights indicated by the color bar. Dotted lines show the predicted transition curves at which the traveling wave is born, as obtained from Eq. (15).

oppose them. Lowering p then yields a discontinuous and hysteretic return to the incoherent state.

On the other hand, if the conformists are more intensely influenced by the mean field ($Q < 1$), the transitions become continuous and reentrant. Figure 3 shows that as p increases from 0, the system goes from incoherence to the π state, then to the traveling wave state and finally back to the π state.

The traveling wave state does not occur in the original Kuramoto model (the limiting case for which $p = 1$) [11] or in the opposite limit $p = 0$ where all the interactions are repulsive [13]. Traveling waves appear only in an intermediate range of p, indicating that both types of oscillators are essential, and only if γ is sufficiently small, indicating that the oscillators need to be close enough to identical. To quantify this, Fig. 4 plots the wave speed $\Omega \equiv (1/N) \times \sum_{j=1}^{N} \langle \dot{\phi}_j \rangle_t$ as a function of p and γ. Notice that the traveling wave state occurs in a wider window as γ tends to 0.

To explain these numerical findings, we begin by reducing the model to a low-dimensional system that governs its long-term macroscopic behavior. As $N \to \infty$, the evolution of the system is given by the continuity equation for the probability density function $f(\phi, K, \omega, t)$:

$$\frac{\partial f}{\partial t} + \frac{\partial}{\partial \phi}(fv) = 0. \tag{4}$$

Here, $v = v(\phi, K, \omega, t)$ is the continuum limit of Eq. (1):

$$v = \omega + K \int \sin(\phi' - \phi) f(\phi', K', \omega', t) \times \Gamma(K') dK' d\phi' d\omega'. \tag{5}$$

The complex order parameter becomes $Z(t) = \int e^{i\phi'} f(\phi', K', \omega', t) \Gamma(K') dK' d\phi' d\omega'$, and the velocity v simplifies to

$$v = \omega + \frac{K}{2i}(Ze^{-i\phi} - \bar{Z}e^{i\phi}), \tag{6}$$

where the overbar indicates the complex conjugate (c.c.). Next we use the remarkable ansatz recently discovered by Ott and Antonsen [14]. The special family of density functions given by

$$f(\phi, K, \omega, t) = \frac{g(\omega)}{2\pi}\left\{1 + \left[\sum_{n=1}^{\infty} [a(K, \omega, t)]^n e^{in\phi} + \text{c.c.}\right]\right\} \tag{7}$$

solves the governing equations exactly, as long as a evolves according to

$$\dot{a} = -i\omega a + \frac{K}{2}(\bar{Z} - Za^2). \tag{8}$$

(This can be checked by substituting Eqs. (6) and (7) into Eq. (4).) Meanwhile, Z reduces to $Z(t) = \int_{-\infty}^{\infty} \int_{-\infty}^{\infty} \Gamma(K) \bar{a}(K, \omega, t) g(\omega) d\omega dK$ since only $n = 1$ in the c.c. term of f contributes to the ϕ integral. A further reduction occurs because $g(\omega)$ is Lorentzian; by closing the contour for the ω integral in the lower half plane, we find $Z(t) = \int_{-\infty}^{\infty} \Gamma(K) \bar{a}(K, -i\gamma, t) dK$. Next, let $z(K, t) = a(K, -i\gamma, t)$. Then Eq. (8) gives

$$\dot{z} = -\gamma z + \frac{K}{2}(\bar{Z} - Zz^2), \tag{9}$$

where $Z = \int_{-\infty}^{\infty} \Gamma(K) \bar{z}(K, t) dK$. For the double-delta distribution $\Gamma(K) = (1 - p)\delta(K - K_1) + p\delta(K - K_2)$, Z is simply

$$Z = (1 - p)\bar{z}_1 + p\bar{z}_2, \tag{10}$$

where $z_1 = z(K_1, t)$ and $z_2 = z(K_2, t)$. The variables z_1 and z_2 have nice interpretations: they are complex order parameters for the contrarians and conformists. From Eqs. (9) and (10), they evolve according to

$$\begin{aligned} \dot{z}_1 &= -2\gamma z_1 - Q[(pz_2 + qz_1) - (p\bar{z}_2 + q\bar{z}_1)z_1^2], \\ \dot{z}_2 &= -2\gamma z_2 + (pz_2 + qz_1) - (p\bar{z}_2 + q\bar{z}_1)z_2^2, \end{aligned} \tag{11}$$

where $q = 1 - p$. (For convenience we have also rescaled time; t has been replaced by $K_2 t/2$ and γ by γ/K_2).

The low-dimensional system (11) is guaranteed to capture all the long-term macroscopic behavior of the original model. This follows from a recent theorem of Ott and Antonsen [15], which makes crucial use of the assumption that the oscillators are nonidentical [16]. We have numerically explored the dynamics of z_1 and z_2 by integrating Eq. (11), and find that we can quantitatively reproduce all the findings shown in Figs. 1–4.

The reduced system yields a number of exact results about the three attractors and their bifurcation points. The incoherent state corresponds to the fixed point $z_1 = 0$, $z_2 = 0$. Linearizing (11) about this state shows that incoherence is stable if and only if $p < p_c$, where

$$p_c = \frac{Q + 2\gamma}{Q + 1}. \tag{12}$$

The π-state is born at p_c when incoherence loses stability and gives rise to a circle of fixed points with $R > 0$. All of these are π-states. They are all equivalent, because of the model's rotational symmetry; they differ only by the arbitrary angle Φ, the phase of the complex order parameter. To calculate how they depend on parameters, let $Z = R > 0$, $z_1 < 0$ and $z_2 > 0$, without loss of generality. Solving Eq. (10) for p, we find $p = (R - z_1)/(z_2 - z_1)$. Then the relevant fixed points of Eq. (11) are $z_1 = [\gamma - \sqrt{\gamma^2 + (QR)^2}]/(QR)$ and $z_2 = (-\gamma + \sqrt{\gamma^2 + R^2})/R$. Hence

$$p = \frac{QR^2 - \gamma + \sqrt{\gamma^2 + (QR)^2}}{-\gamma Q + Q\sqrt{\gamma^2 + R^2} - \gamma + \sqrt{\gamma^2 + (QR)^2}}. \quad (13)$$

This gives an exact parametrization of the π-states. Near the transition point where $R \to 0$, we find that $R \sim (p - p_c)^{1/2}$, where $p_c = (Q + 2\gamma)/(Q + 1)$ as before.

The traveling wave state is created when the circle of π-states loses stability and turns into a circular limit cycle for Eq. (11). To calculate this bifurcation, let $z_1 = r_1 e^{-i\psi_1}$ and $z_2 = r_2 e^{-i\psi_2}$. Then Eq. (11) yields

$$\begin{aligned} \dot{r}_1 &= -2\gamma r_1 - Q(1 - r_1^2)(q r_1 + p r_2 \cos\delta), \\ \dot{r}_2 &= -2\gamma r_2 + (1 - r_2^2)(p r_2 + q r_1 \cos\delta), \\ \dot{\delta} &= \sin\delta\left[Qp\frac{r_2}{r_1}(1 + r_1^2) - q\frac{r_1}{r_2}(1 + r_2^2)\right], \end{aligned} \quad (14)$$

where $\delta \equiv \psi_1 - \psi_2$. The advantage is that the traveling wave state reduces to a fixed point of (14), with $\delta \neq \pi$. Linearizing (14) about the π-state (13) and seeking a zero eigenvalue, we find that for $\gamma \ll 1$ the transition to the traveling wave state occurs at

$$\begin{aligned} p_\ell &= \frac{Q}{1 + Q} + \frac{3\gamma}{1 + Q} + O(\gamma^{3/2}), \\ p_u &= \frac{1}{1 + Q} - \frac{\gamma}{1 + Q} + \frac{(Q + 1)\gamma^2}{(Q - 1)Q} + O(\gamma^3), \end{aligned} \quad (15)$$

where p_ℓ and p_u represent the lower and upper values at which the π state loses stability. These predicted stability boundaries, shown as dotted curves in Fig. 4, are in good agreement with the simulation results. The theory also correctly predicts that if γ is large enough, the traveling wave state disappears and π state becomes stable for all R. For instance, when $Q = 0.5$, a numerical eigenvalue computation shows that the π state is always stable if $\gamma \gtrsim 0.06$, as in Fig. 4.

In future work, it will be interesting to see if the traveling wave also occurs in models with local coupling. Its existence in the present model is made possible by the asymmetry of the coupling: $K_{ij} \neq K_{ji}$. Such asymmetry is common in biological and social systems. For experimental tests of the model's predictions, however, it might be more promising to look for physical realizations of Eq. (3) in series arrays of Josephson junctions [19] or in liquid crystal spatial light modulators suitably coupled by global optoelectronic feedback [20].

Research supported by the LG YONAM Foundation (H. H.) and NSF Grant CCF-0835706 (S. H. S.). We thank R. Roy and K. Wiesenfeld for their helpful comments.

[1] A. T. Winfree, *The Geometry of Biological Time* (Springer, New York, 1980); Y. Kuramoto, *Chemical Oscillations, Waves, and Turbulence* (Springer, Berlin, 1984); J. A. Acebron *et al.*, Rev. Mod. Phys. **77**, 137 (2005).
[2] H. Daido, Prog. Theor. Phys. **77**, 622 (1987); Phys. Rev. Lett. **68**, 1073 (1992); L. L. Bonilla *et al.*, J. Stat. Phys. **70**, 921 (1993); D. H. Zanette, Europhys. Lett. **72**, 190 (2005).
[3] D. Sherrington and S. Kirkpatrick, Phys. Rev. Lett. **35**, 1792 (1975).
[4] J. C. Stiller and G. Radons, Phys. Rev. E **58**, 1789 (1998); H. Daido, Phys. Rev. E **61**, 2145 (2000); J. C. Stiller and G. Radons, Phys. Rev. E **61**, 2148 (2000).
[5] C. Börgers and N. Kopell, Neural Comput. **15**, 509 (2003).
[6] G. H. Paissan and D. H. Zanette, Physica (Amsterdam) **237D**, 818 (2008).
[7] H. Hong and S. H. Strogatz (to be published).
[8] S. Galam, Physica (Amsterdam) **333A**, 453 (2004); M. S. Lama, J. M. López, and H. S. Wio, Europhys. Lett. **72**, 851 (2005).
[9] E. A. Martens *et al.*, Phys. Rev. E **79**, 026204 (2009).
[10] D. M. Abrams, R. Mirollo, S. H. Strogatz, and D. A. Wiley, Phys. Rev. Lett. **101**, 084103 (2008).
[11] Traveling waves were previously seen in a variant of the Kuramoto model where a phase shift term breaks the odd symmetry of the original sine coupling function [12]. In contrast our model retains the odd symmetry, so the traveling waves come in symmetric pairs, with frequencies $\pm\Omega$. They stem from the asymmetry in the coupling parameters K_i, not in the coupling function itself.
[12] H. Sakaguchi and Y. Kuramoto, Prog. Theor. Phys. **76**, 576 (1986).
[13] L. S. Tsimring, N. F. Rulkov, M. L. Larsen, and M. Gabbay, Phys. Rev. Lett. **95**, 014101 (2005).
[14] E. Ott and T. M. Antonsen, Chaos **18**, 037113 (2008).
[15] E. Ott and T. M. Antonsen, Chaos **19**, 023117 (2009).
[16] The theorem does not apply when $\gamma = 0$. The identical case displays states not described by the ansatz above, such as a large manifold of neutrally stable states [17], as seen in other systems [18].
[17] H. Hong and S. H. Strogatz (to be published).
[18] A. Pikovsky and M. Rosenblum, Phys. Rev. Lett. **101**, 264103 (2008); S. A. Marvel and S. H. Strogatz, Chaos **19**, 013132 (2009).
[19] K. Wiesenfeld, P. Colet, and S. H. Strogatz, Phys. Rev. E **57**, 1563 (1998).
[20] E. A. Rogers *et al.*, Phys. Rev. Lett. **93**, 084101 (2004).